Electronic Supplemental Information (ESI)

Title

Soft Nanotubes Acting as a Confinement Effecter and a Chirality Inducer for Achiral Polythiophenes

Authors

Naohiro Kameta,* Mitsutoshi Masuda, and Toshimi Shimizu

1. Synthesis of PolyT-B(OH)$_2$ with two-different molecular-weight distributions

The synthesis was carried out according to our published paper*. The molecular weights were estimated by size exclusion chromatography (SEC).

*N. Kameta, K. Ishikawa, M. Masuda, T. Shimizu, *Langmuir*, 2013, **29**, 13291.

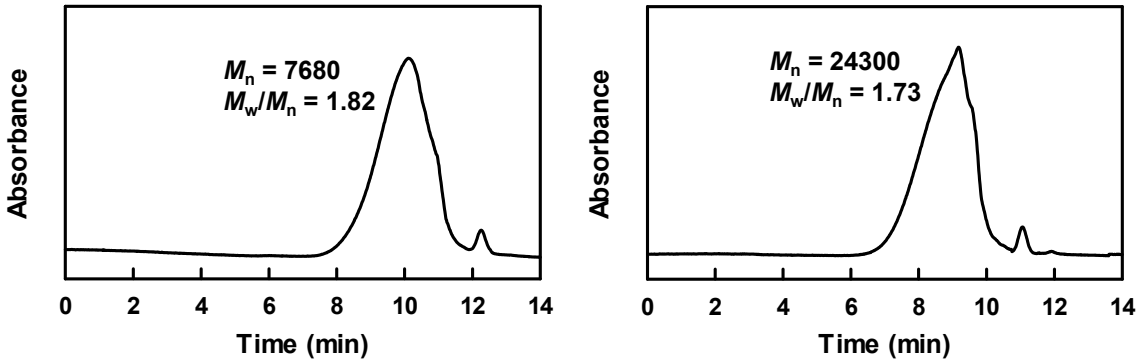

Fig. S1 SEC charts of PolyT-B(OH)$_2$. Column: KF-803 (Shodex), Eluent: THF, Flow Rate: 1.0 mL/min

2. Construction of nanotubes with three-different inner diameters

2-1. Morphological observation 1 eq. NaOH was added to the water/DMSO (v/v = 90/10) dispersions of Tgly (5.0 mg, 8.5 μmol) and either Dgly (4.5 mg, 8.5 μmol) or Mgly (4.0 mg, 8.5 μmol) at room temperature. The resultant dispersions were dropped onto carbon grids, and the grids were dried under vacuum conditions. TEM (Hitachi H7000, 75 kV) observations showed that the co-assembly gave mixtures of the nanotubes and nanofibers.

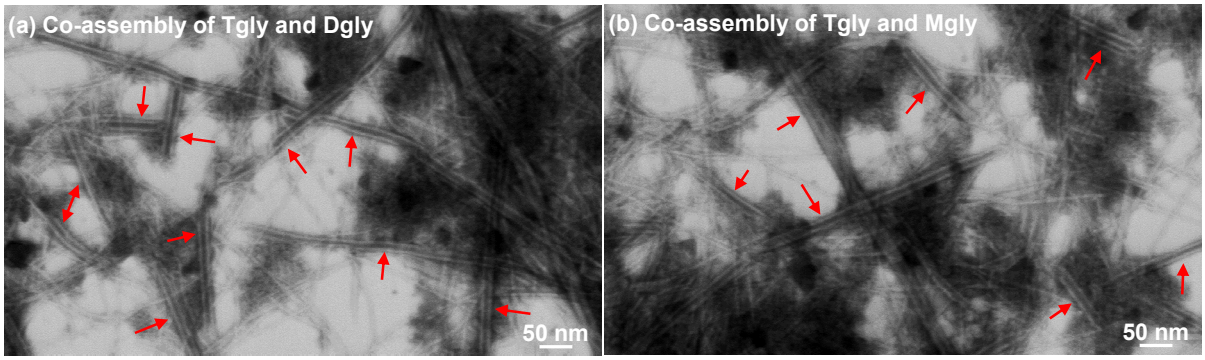

Fig. S2 TEM images of the mixtures of the nanotubes (arrows) and nanofibers (other objects without arrows) formed by co-assembly of Tgly and Dgly or MGly. The nanotube channels were visualized with 2wt% phosphotungstate as a negative staining reagent.

2-2. Molecular packing analysis by IR spectroscopy The $\delta(CH_2)$ scissoring vibration bands reflecting the lateral chain packing of the oligomethylene spacer in the wedge-shaped glycolipids, the so-called "subcell structure" support the difference in the molecular packing of the nanotubes and nanofibers. A single sharp peak of each band at 1465 cm^{-1} for the nanotubes indicates a triclinic parallel ($T_{//}$) structure. A single broad peak of each band for the nanofibers is compatible with a distorted hexagonal (Hex) structure. The latter case allows the coexistence of the antiparallel molecular packing due to the incomplete hydrogen-bond network among mono- and di-glycine moieties. In fact, the frequencies of the C=O stretching (amide I) and N-H deformation (amide II) bands support the view that the amide hydrogen bond of the nanotubes was stronger than that of the nanofibers.

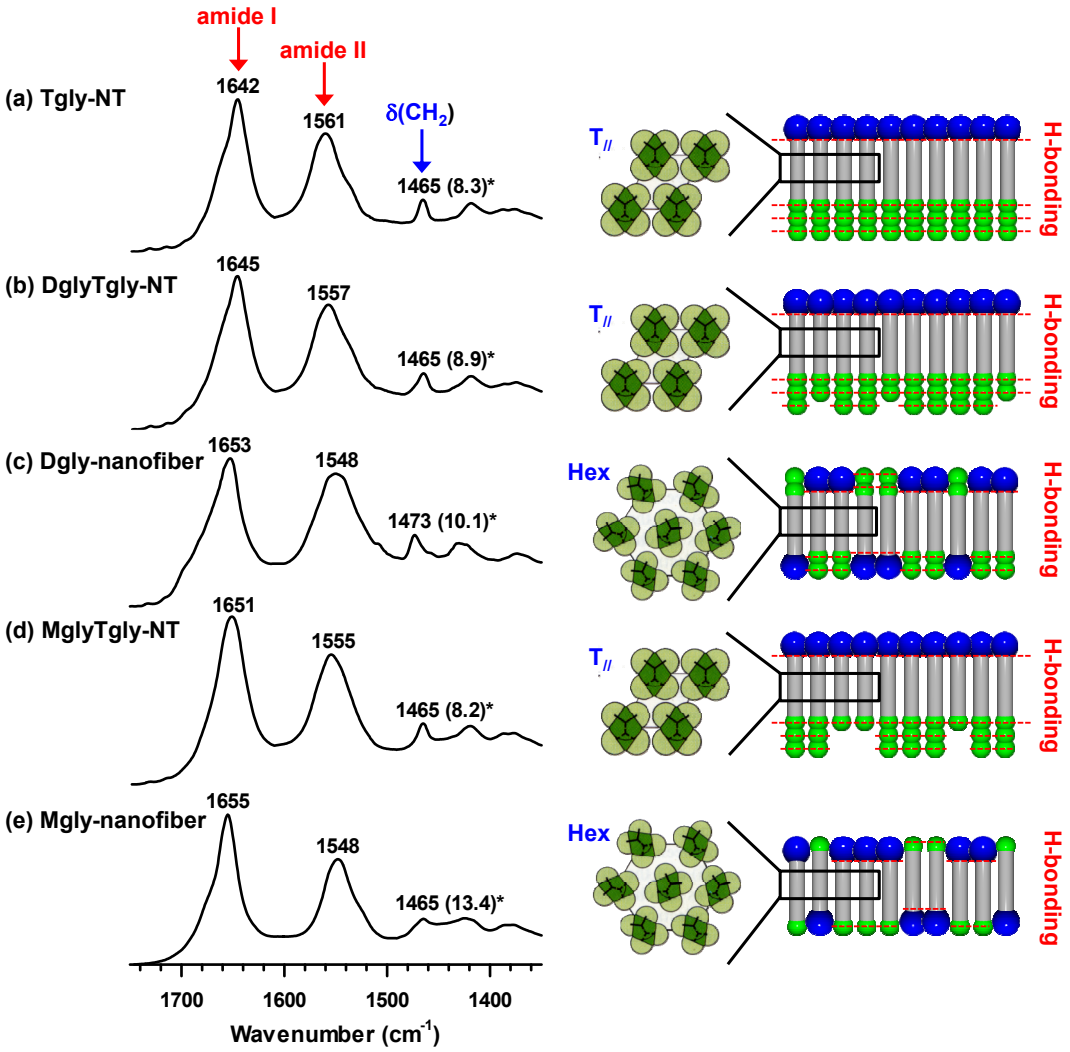

Fig. S3 IR spectra for the amide-I, amide-II and CH_2 scissoring bands of the nanotubes and nanofibers. The parenthesis ( )* means a full width half-maximum. Schematic images are shown for the subcell structures of the oligomethylene spacer within the monolayer membranes and the intermolecular hydrogen-bonding among glucose moieties and oligoglycine moieties.

2-3. Molecular packing analysis by CD spectroscopy Based on elastic theory, two different types of formation mechanisms for soft nanotubes have been proposed and well-documented in theoretical and experimental view points: chiral self-assembly (mechanism A) and packing-directed self-assembly (mechanism B).* According to the mechanism A, molecular chirality causes the constituent amphiphilic molecules to pack at a nonzero angle with respect to their nearest neighbors within their membrane, and then induces single particular orientation when the molecules tilt. This packing eventually causes the membrane twisting or coiling to form helical tapes as intermediate morphologies, and some of the intermediates are finally transformed into nanotubes. The mechanism B proposes that wedge-shaped amphiphilic molecules have tendency to form spray type packing and then induce spontaneous bending of their membrane, and finally form hollow cylinder structures. The latter mechanism works only when the molecules packed in a parallel fashion and had shallow tilt with respect to the membrane surface.

The present all nanotubes had negative and positive cotton bands in the CD spectra. The wavelength region displaying the cotton effect corresponds to the absorption band of conjugated amide linkages in the assembly of Tgly and the co-assembly of Tgly with Dgly or Mgly. The CD intensities of the each nanotube were larger than that of the molecules themselves, indicating that the chirality of the molecules is amplified through the nanotube formation based on the twist packing (chiral packing). The enhancement of the CD intensities increased in the order of Tgly-NT < DglyTgly-NT < MglyTgly-NT. These results suggest that the twist packing and the spray packing should be dominant factors for the formations of the MglyTgly-NT and the Tgly-NT, respectively.

*T. Shimizu, M. Masuda, H. Minamikawa, *Chem. Rev.* 2005, **105**, 1401.

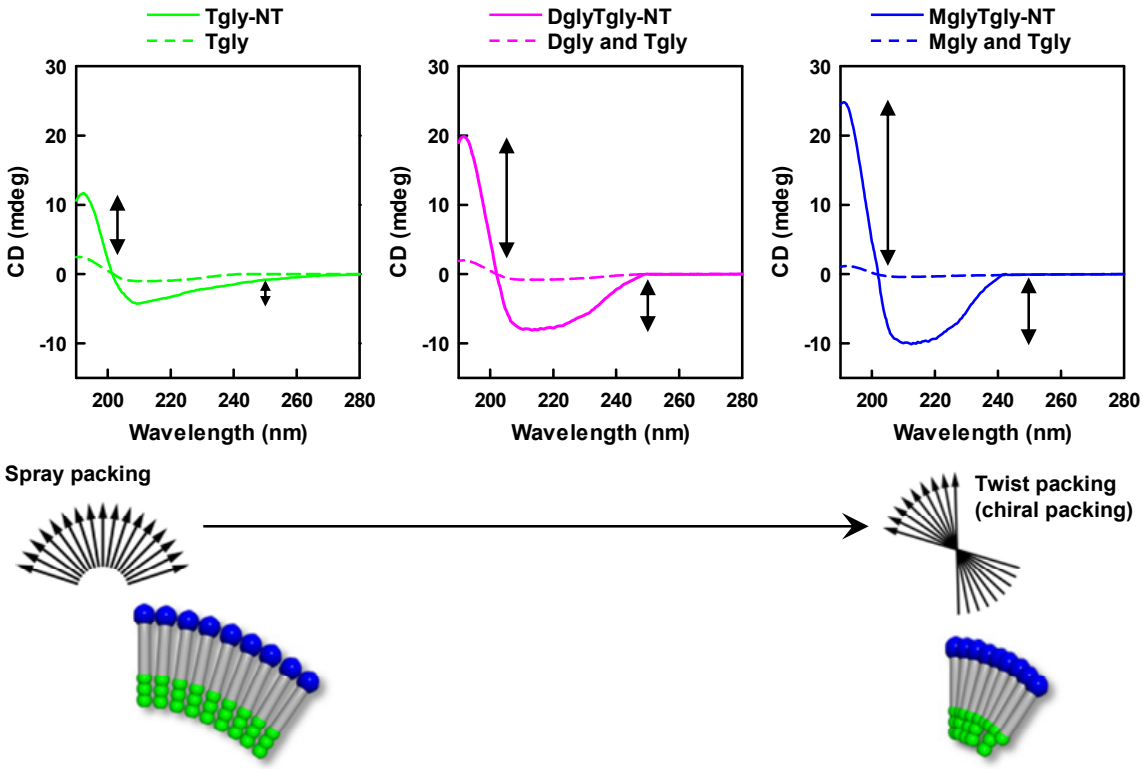

Fig. S4 (Solid lines) CD spectra of the Tgly-NT, DglyTgly-NT and MglyTgly-NT in water/DMSO (v/v = 90/10) at 25 °C. The concentrations of each nanotube are 1.2×10^{-4} M. (Dotted lines) CD spectra of Tgly, Dgly and Mgly existing as molecules obtained from thermal destruction of the nanotubes in water/DMSO (v/v = 90/10) at 60 °C. Schematic image of the spry packing and the twist packing (chiral packing).

3. Determination of encapsulation ratio of PolyT-B(OH)$_2$ in the nanotube channels

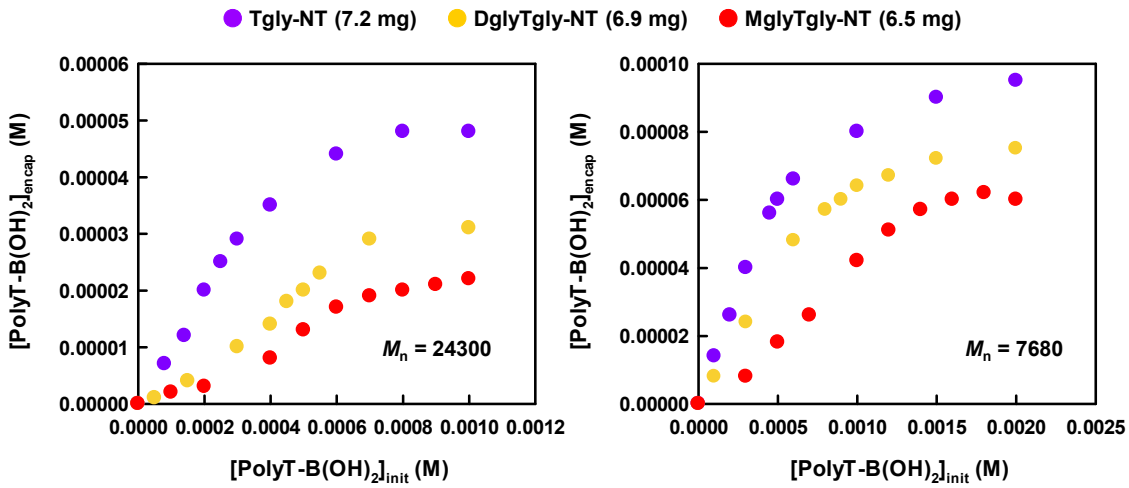

Fig. S5 Relationship between the initial concentrations of the used PolyT-B(OH)$_2$ and the concentration of the encapsulated PolyT-B(OH)$_2$ in the nanotubes. The encapsulation method

and the determination method are as follows: Single component of Tgly, two components of Tgly and Dgly or Tgly and Mgly were dispersed in 2 ml water/DMSO (v/v = 90/10) at room temperature. After addition of PolyT-B(OH)$_2$ into the dispersions, the neutralization using 1 eq. NaOH was carried out to form the nanotubes. The resultant dispersions were filtered by using polycarbonate membranes with 0.2 μm pore size. The residual nanotubes were washed by the same solvents for several times to remove non-encapsulated PolyT-B(OH)$_2$. Destruction of the nanotubes by heating at 60 °C for 1 min in the presence of 1 eq. HCl and then cooling to room temperature allowed us to determine the concentration of the encapsulated PolyT-B(OH)$_2$ by absorption spectroscopy.

4. Determination of release ratio of the encapsulated PolyT-B(OH)$_2$ to the bulk solution

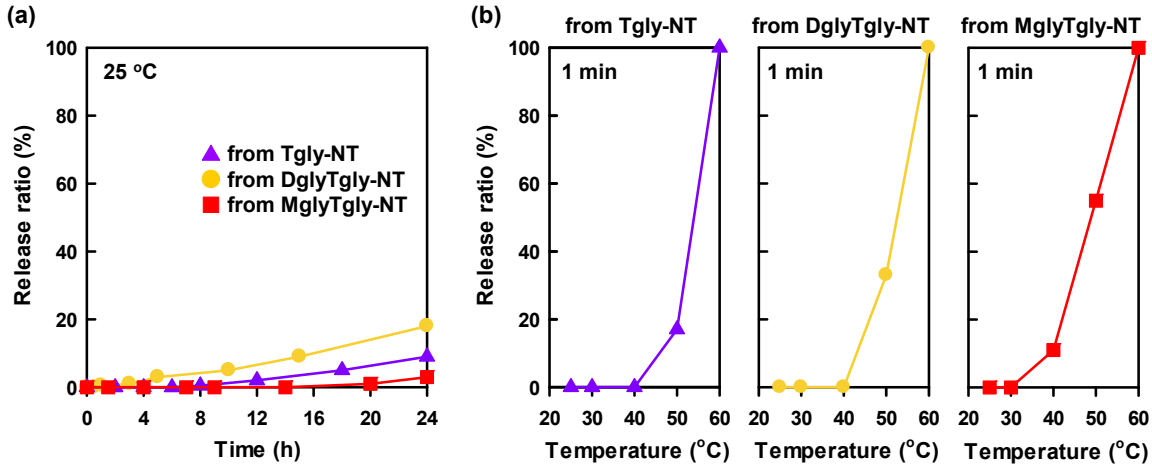

Fig. S6 (a) Time dependence of the release ratio of PolyT-B(OH)$_2$ (M_n = 24300) from the nanotubes to the bulk solutions at 25 °C under pH 7.4–7.8 conditions. (b) Temperature dependence of the release ratio of PolyT-B(OH)$_2$ (M_n = 24300) from the nanotubes to the bulk solutions under pH 5.8–6.2 conditions. Incubation time after elevating temperature was 1 min. The enhancements of the release ratio are ascribable to the compulsive release caused by the destruction of the nanotubes.

5. Conformational analysis of the encapsulated PolyT-B(OH)$_2$ in the nanotube channels

The solid-state sample of PolyT-B(OH)$_2$ prepared from the solution-dispersed sample of free PolyT-B(OH)$_2$, which has an absorption band at 404 nm ((a) a green solid line) assignable to the random-coil conformation, had a red-shifted absorption band at 542 nm and two shoulders ((a) a black dotted line) assignable to strong non-specific aggregation. In contrast, essentially no difference in the absorption spectra was observed between the solid-state samples ((b, c, d) dotted lines) and the solution-dispersed samples ((b, c, d) solid lines) of encapsulated PolyT-B(OH)$_2$ in the nanotubes. These results indicate that PolyT-B(OH)$_2$ does not exist on the outer surface of the nanotubes and never form the strong non-specific aggregation by complete isolation in the nanotube channels.

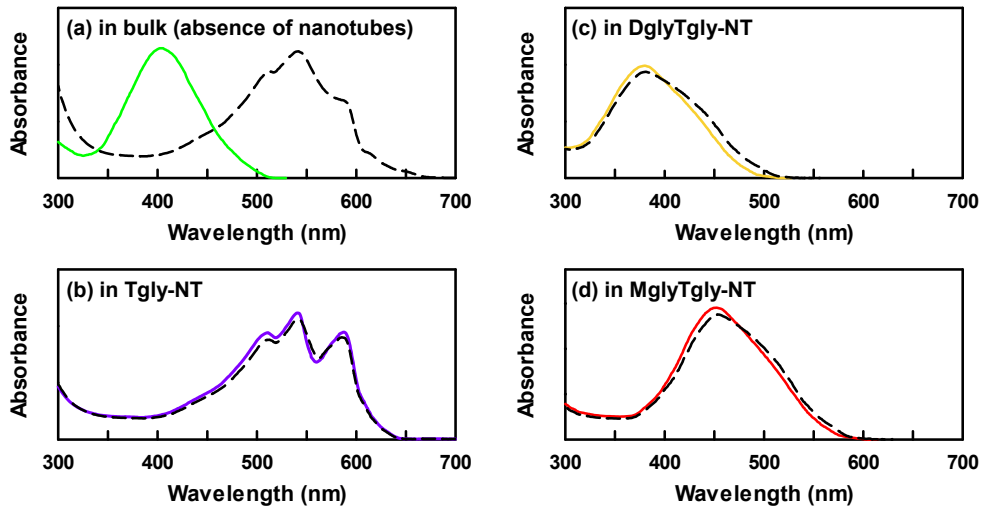

Fig. S7 Absorption spectra of the solid films (dotted lines) of the PolyT-B(OH)$_2$ (M_n = 24300) and the encapsulated PolyT-B(OH)$_2$ in the nanotubes, and their dispersions (solid lines) in water/DMSO (v/v = 90/10).

The nanotubes were able to not only control the conformation of PolyT-B(OH)$_2$ with a smaller molecular weight (M_n = 7680) by the encapsulation in the nanochannels but also induce the chirality for the encapsulated PolyT-B(OH)$_2$, depending on their inner diameters. The conformation type and the Cotton effect patterns of the encapsulated PolyT-B(OH)$_2$ with M_n = 7680 were similar to those of the encapsulated one with M_n = 24300, although the maximal absorption wavelength was different each other because of the difference in the effective conjugation lengths.

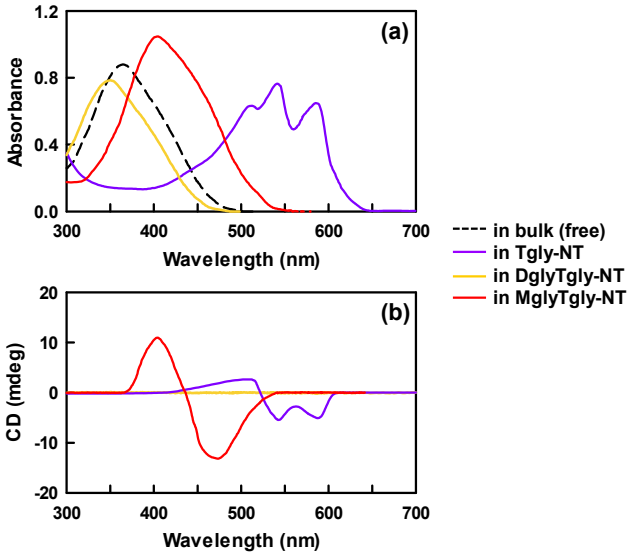

Fig. S8 (a) Absorption spectra and (b) CD spectra of 6.0×10^{-5} M free PolyT-B(OH)$_2$ (M_n = 7680) in water/DMSO (v/v = 90/10) and 6.0×10^{-5} M the encapsulated PolyT-B(OH)$_2$ in the nanotube channels dispersed in water/DMSO (v/v = 90/10).

The L-MglyTgly-NT, self-assembled from the enantiomers (having a L-glucose unit) of Mgly and Tgly, showed an opposite directional Cotton effects against those of the MglyTgly-NT. Reflecting the difference of chirality between both nanotubes, the encapsulated PolyT-B(OH)$_2$ in the both nanotubes gave almost symmetrical induced CD patterns, which are characteristic of the left- and right-handed helicity in the MglyTgly-NT and L-MglyTgly-NT, respectively.

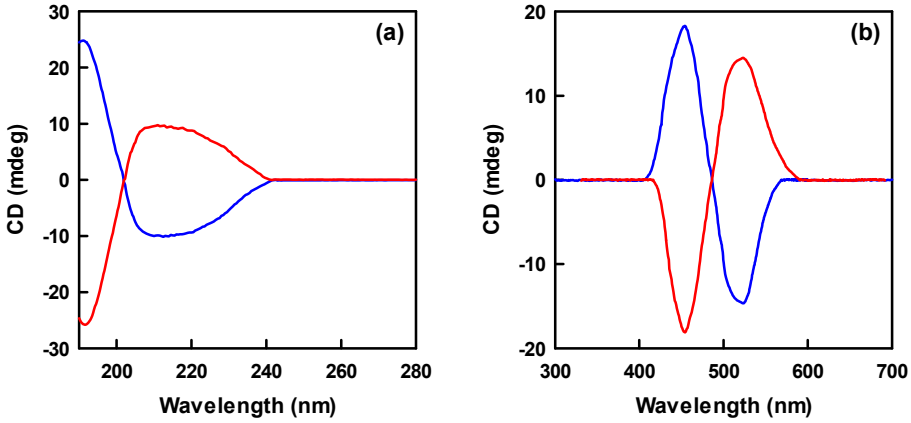

Fig. S9 (a) CD spectra of 1.2×10^{-4} M the MglyTgly-NT (blue line) and L-MglyTgly-NT (red line) in water/DMSO (v/v = 90/10). (b) CD spectra of 6.0×10^{-5} M the encapsulated PolyT-B(OH)$_2$ (M_n = 24300) in the MglyTgly-NT (blue line) and L-MglyTgly-NT (red line) dispersed in water/DMSO (v/v = 90/10).

6. Evaluation for the recognition ability of PolyT-B(OH)$_2$ toward D, L-sugars and Tgly

Aromatic boronic acids often play the role of a fluorescent probe for diol compounds including carbohydrates.* The fluorescence band of PolyT-B(OH)$_2$ was sharply decreased by association with D, L-glucose, D, L-galactose and D, L-fructose in water/DMSO (v/v = 90/10). On the other hand, the fluorescence band of PolyT-B(OH)$_2$ was no changed in the presence of Mgly, Dgly and Tgly because of its poor complexation with glucose moieties without 1-OH group in the glycolipids.

*T. D. James et al., *Angew. Chem. Int. Ed.* 1996, **35**, 1910.

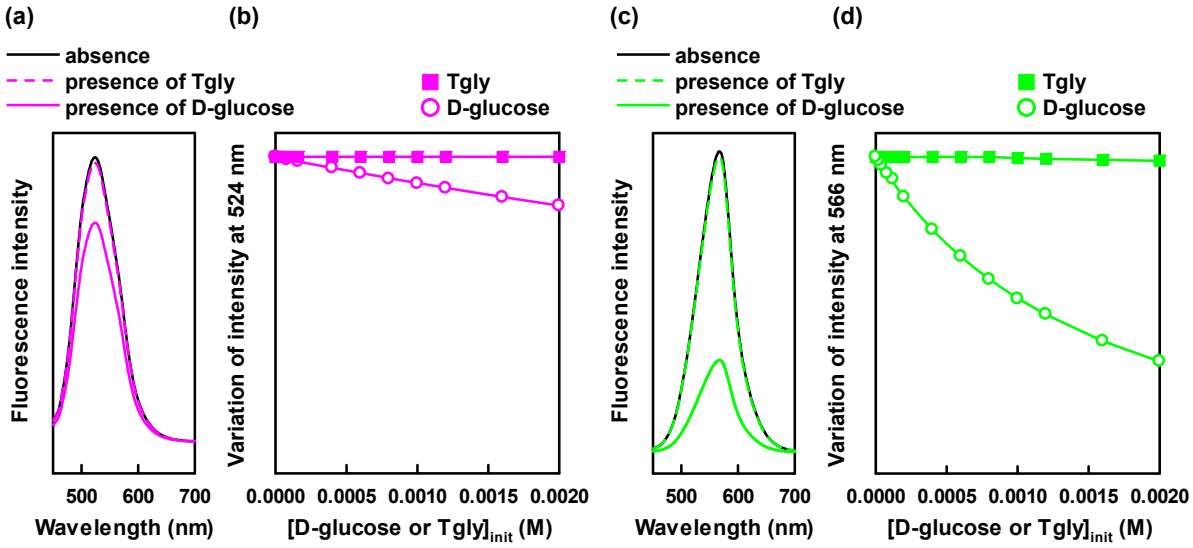

Fig. S10 (a) Fluorescence spectra of 2.0×10^{-5} M free PolyT-B(OH)$_2$ (M_n = 24300) in water/DMSO (v/v = 90/10) in the presence and absence of 2.0×10^{-3}M D-glucose or Tgly at pH 5.8–6.2 (b) Relationship between the variation of the fluorescence intensity at 524 nm and the initial concentration of D-glucose or Tgly. (c) Fluorescence spectra of 2.0×10^{-5} M the released PolyT-B(OH)$_2$ (M_n = 24300) from the MglyTgly-NT to water/DMSO (v/v = 90/10) in the presence and absence of 2.0×10^{-3}M D-glucose or Tgly at pH 5.8–6.2. The release was caused by the thermal destruction of the MglyTgly-NT as described above. (d) Relationship between the variation of the fluorescence intensity at 566 nm and the initial concentration of D-glucose or Tgly.

7. Evaluation for the chiral memory of the released PolyT-B(OH)$_2$ from the MglyTgly-NT into the bulk solution

Upon heating at 60 ^{o}C for 1 min in the presence of 1 eq. HCl, the encapsulated PolyT-B(OH)$_2$ was compulsively released from the MglyTgly-NT or the Tgly-NT to the bulk solution, and both nanotubes completely disassembled. The disassembled components, Mgly and Tgly, or only Tgly, were removed from the systems by precipitation using THF.

As soon as the disassembly of the Tgly-NT, the red-shifted absorption band with three peaks at 511, 541 and 587 nm of the PolyT-B(OH)$_2$ aggregates was returned to the wavelength region (at 404 nm) of free PolyT-B(OH)$_2$ with the random-coil conformation (Figure S11a, b). The induced CD was rapidly disappeared in conjunction with the above conformational change (Figure S11c, d).

On the other hand, the red-shifted absorption band at 452 nm of the released PolyT-B(OH)$_2$ from the MglyTgly-NT was retained for some time, returning to the wavelength region (at 404 nm) of free PolyT-B(OH)$_2$ with the random-coil conformation after 3 h (Figure S11e, f). The induced CD was also retained for some time, disappearing after 3 h (Figure S11g, h). The appearance of such chiral memory will be attributable to self-association among the released PolyT-B(OH)$_2$ from the MglyTgly-NT, since the released PolyT-B(OH)$_2$ to the bulk solution in the absence of the chiral sources should be difficult to completely keep the chiral conformation, i.e., one-dimensional planer conformation with the left-handed helicity, induced by encapsulation in the MglyTgly-NT. The disappearance of the chiral memory after 3 h can be related to dissociation of the self-associated PolyT-B(OH)$_2$. However, the red-shifted absorption spectrum and the induced CD spectrum of the released PolyT-B(OH)$_2$ to the bulk solution were similar to those of the encapsulated PolyT-B(OH)$_2$ in the MglyTgly-NT, suggesting that the released PolyT-B(OH)$_2$ still keeps partly the planer conformation even after it forms the self-association, which is distinguishable from the aggregation in the Tgly-NT system.

To support the chiral memory phenomenon, Mgly and Tgly or those enantiomers (excess amounts against the amounts used for the nanotube formation) were re-added into the released PolyT-B(OH)$_2$ in the bulk solution. The sustainability of the chiral memory was never influenced by those chiral sources (red cross plots in Fig. S11h).

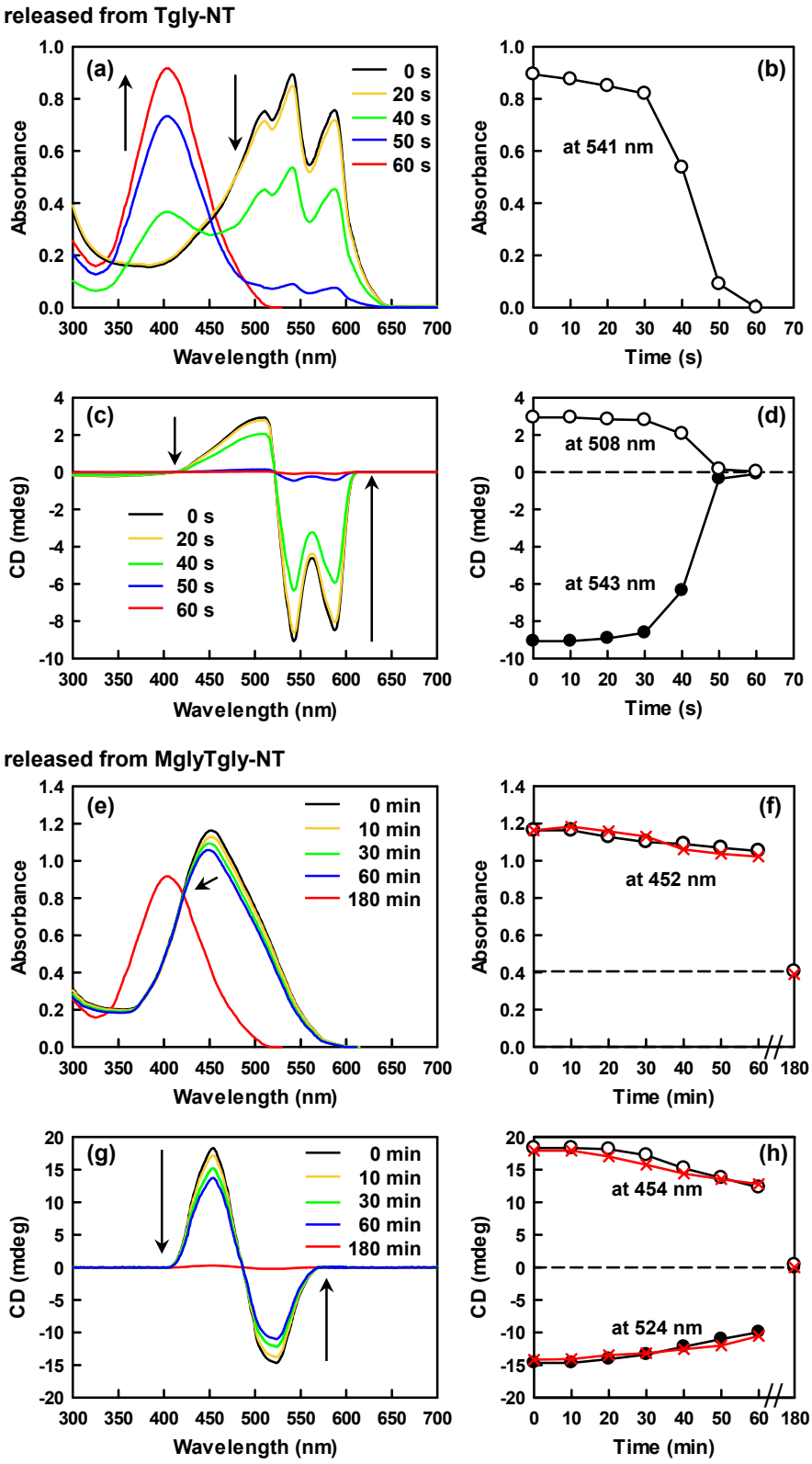

Fig. S11 Variation of (a, e) the absorption spectra, (b, f) the absorbance, (c, g) the CD spectra and (d, h) the CD intensities of the released PolyT-B(OH)$_2$ in water/DMSO/THF (v/v/v = 82/9/9) from the nanotubes. The nanotubes were destructed by heating at 60 ^{o}C for 1 min in the presence of 1 eq. HCl, and then the disassembled components, Mgly and Tgly, were precipitated by addition of THF. Red cross plots: presence of enantiomers of Mgly and Tgly.

8. Determination of association constants of free PolyT-B(OH)$_2$, the encapsulated PolyT-B(OH)$_2$ in the MglyTgly-NT or DglyTgly-NT and the released PolyT-B(OH)$_2$ from the MglyTgly-NT with D,L-sugars

Samples were prepared by addition of PolyT-B(OH)$_2$ or freeze-dried nanotubes encapsulating PolyT-B(OH)$_2$ into the water/DMSO (v/v = 90/10) solution of D-sugars or L-sugars at pH 8.6–9.2, which are adjusted by NaOH. Capillary force* enabled the nanotubes to encapsulate D-sugars or L-sugars in the nanochannel existing PolyT-B(OH)$_2$. Each sample was subjected to following fluorescence spectroscopy. Release of the encapsulated PolyT-B(OH)$_2$ into the bulk solution was ignored under given experimental conditions (Fig. S6, ESI). On the other hand, upon heating at 60 ^{o}C for 1 min in the presence of 1 eq. HCl, the nanotubes completely disassembled, and the encapsulated PolyT-B(OH)$_2$ was compulsively released from the nanotubes to the bulk solution. THF was added into the solution to precipitate the nanotube components, Mgly (or Dgly) and Tgly. The supernatant including the released PolyT-B(OH)$_2$ in water/DMSO/THF (v/v/v = 82/9/9) solution was used for following fluorescence spectroscopy.

As shown in Fig. S10, ESI, PolyT-B(OH)$_2$ act as the fluorescent probe for sugars. The fluorescence intensity of PolyT-B(OH)$_2$ sharply decreased by association with D, L-glucose, D, L-galactose and D, L-fructose in water/DMSO (v/v = 90/10) or water/DMSO/THF (v/v/v = 82/9/9) at pH 8.6–9.2. The association constants were determined by applying a nonlinear least-squares method based on the Benesi–Hildebrand equation to the variation of fluorescence intensity.

*T. Shimizu, *J. Polym. Sci. Part A* 2008, **46**, 2601.

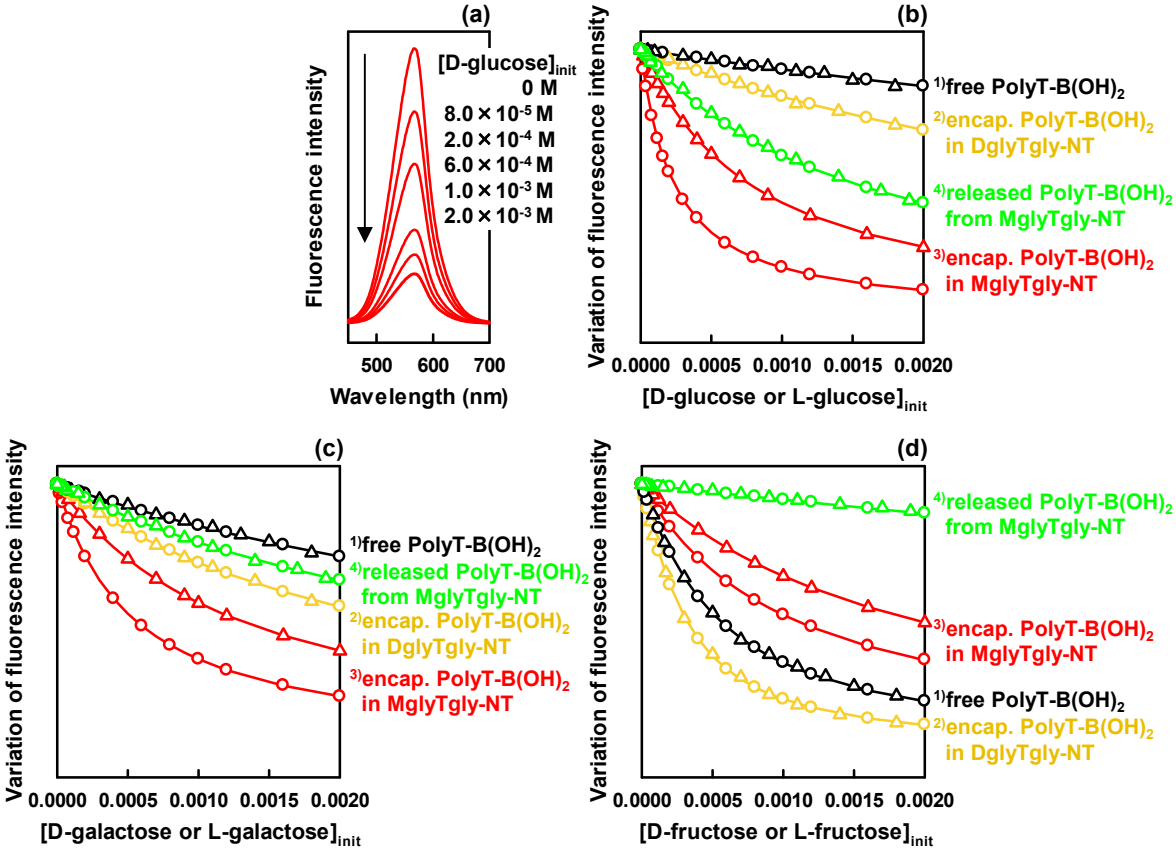

Fig. S12 (a) Fluorescence spectra of PolyT-B(OH)$_2$ (2.0×10^{-5} M) encapsulated in MglyTgly-NT in the presence and absence of D-glucose (0–2.0×10^{-3} M) in water/DMSO (v/v = 90/10) at pH 8.6–9.2. (b, c, d) Variation of the fluorescence intensity at the maximum fluorescence wavelength of free PolyT-B(OH)$_2$, the encapsulated PolyT-B(OH)$_2$ in the DglyTgly-NT or MglyTgly-NT and the released PolyT-B(OH)$_2$ from the MglyTgly-NT against the initial concentration of D-sugars (○) or L-sugars (△). Solid lines are fitting curves calculated by using the obtained association constants. Solutions: [1)2)3)]water/DMSO (v/v = 90/10) at pH 8.6–9.2; [4)]water/DMSO/THF (v/v/v = 82/9/9) at pH 8.6–9.2.

Table S1 Association constants (K / (M^{-1})) of PolyT-B(OH)$_2$ with D, L-sugars

PolyT-B(OH)$_2$	Glucose		Galactose		Fructose	
	D form / L form	K_D / K_L	D form / L form	K_D / K_L	D form / L form	K_D / K_L
[a]free in bulk	$\frac{8.0\times10}{8.0\times10}$	1.0	$\frac{1.9\times10^2}{1.9\times10^2}$	1.0	$\frac{2.3\times10^3}{2.3\times10^3}$	1.0
[b]encapsulated in DglyTgly-NT	$\frac{2.2\times10^2}{2.2\times10^2}$	1.0	$\frac{4.4\times10^2}{4.4\times10^2}$	1.0	$\frac{4.8\times10^3}{4.8\times10^3}$	1.0
[c]encapsulated in MglyTgly-NT	$\frac{4.4\times10^3}{1.5\times10^3}$	2.9	$\frac{1.9\times10^3}{8.7\times10^2}$	2.2	$\frac{9.6\times10^2}{5.6\times10^2}$	1.7
[d]released from MglyTgly-NT	$\frac{7.1\times10^2}{7.1\times10^2}$	1.0	$\frac{2.9\times10^2}{2.9\times10^2}$	1.0	$\frac{6.2\times10}{6.2\times10}$	1.0

Conformation of PolyT-B(OH)$_2$: [a)b)]random-coil; [c]one-dimensional planer

Solutions: [a)b)c)]water/DMSO (v/v = 90/10); [d]water/DMSO/THF (v/v/v = 82/9/9)

Table S2 Association constants (K / (M^{-1})) of PolyT-B(OH)$_2$ with D, L-sugars

PolyT-B(OH)$_2$	Glucose		Galactose		Fructose	
	D form / L form	K_D / K_L	D form / L form	K_D / K_L	D form / L form	K_D / K_L
[a]encapsulated in MglyTgly-NT*	$\frac{4.4\times10^3}{1.5\times10^3}$	2.9	$\frac{1.9\times10^3}{8.7\times10^2}$	2.2	$\frac{9.6\times10^2}{5.6\times10^2}$	1.7
[b]encapsulated in L-MglyTgly-NT**	$\frac{1.4\times10^3}{4.2\times10^3}$	1.0 / 3.0	$\frac{8.5\times10^2}{1.7\times10^3}$	1.0 / 2.0	$\frac{5.8\times10^2}{9.8\times10^2}$	1.0 / 1.7

*self-assembled from Mgly and Tgly **self-assembled from enantiomers of Mgly and Tgly

Conformation of PolyT-B(OH)$_2$: [a)b)]one-dimensional planer

Solutions: [a)b)]water/DMSO (v/v = 90/10)